IOSR Journal of Applied Chemistry (IOSR-JAC)
e-ISSN: 2278-5736.Volume 16, Issue 3 Ser. I (March 2023), PP 33-39
www.iosrjournals.org

Synthesis of Bismuth Selenide nanoparticles and its Photocatalytic activity for the degradation of some textile dyes

M.Shanti[1,2], U.UmeshKumar[3*]
[1,3](Department of Chemistry, University College of Science, Osmania University, Tarnaka,Hyderabad-500007,T. S,India)
[2](G.NarayanammaInstitute ofTechnologyScience,Hyderabad-500104,T. S,India)
*For Correspondence: utkoor@gmail.com

Abstract:
In the current study, Bi_2Se_3 nanoparticles are prepared under greenery conditions using economically viable desktop chemicals such as L-Ascorbic acid (vitamin C), $BiCl_3$, EDTA (Ethylene diamine tetra acetic disodium salt) and sodium selenite (Na_2SeO_3). Prepared Bi_2Se_3 nanoparticles were characterized by XRD (X-ray Diffraction), Scanning electron microscopy (SEM), EDAX,UV-Visible, and TEM studies. Prepared nanocatalyst is found as an efficient catalyst for photodegradation of cationic dyes . The effect of catalyst morphology on dye degradation and the photocatalytic efficiency of catalysts were evaluated. This study helps to understand the pathway to eliminate highly toxic and persistent cationic dyes.

Key Words*:Dyes, Photodegradation,Bi_2Se_3*

Date of Submission: 05-03-2023 Date of Acceptance: 17-03-2023

I. Introduction

In the present scenario developmental activities have led to increase in the economic status which led to increase in environmental pollution due to addition of poisonous pollutants which is considered to be a serious environmental issue . Everyday diversified pollutants such as organic or inorganic origin are entering into the environment . Since the invention of first dye, Mauveine, by William Henry Perkin in 1856 synthetic dyes are being used extensively in diverse fields [1,2]. Presently, around 0.1 million [3] type of synthetic dyes are being used in various industries like, textile [4], leather [5,6], printing [7], paint [8], paper [9], plastic [10], cosmetics [11], pharmaceuticals [12] ,food [13,14] on daily basis.During processing a large percentage of these dyes are lost and released as waste water[15,16]. Since these synthetic dyes are highly photostable[17] and non-biodegradable[18] in nature remain in the environment for a very long time. Usually dyes in waste water prevent the penetration of sunlight and reduce the amount of dissolved oxygen in water which endangers aquatic life[19]. Different methodologies have been adopted for the removal of dyes from waste water which includes, chemical oxidation, adsorption , biological degradation, membrane filtration and photocatalytic degradation etc [20-24]. Among these photocatalytic degradation is the simplest way out solution for this problem because of low cost effectiveness and easy to implement . Among the bismuth chalcogenides ,bismuth selenide a member of a family V-VI is gaining momentum due to its wide range of applications as thermoelectric devices[25],optical devices[26] topological insulators[27], semiconductors[28].Bismuth based semiconductors have become a promising group of advanced photocatalytic materials[29-30]. In recent years synthesis of BismuthSelenide (Bi_2Se_3) at nanoscale has received quite some attention during the past decades owing to low toxicity ,environmentally friendly element, easily available andeconomical.

II. Experimental Methods

2.1 Synthesisof Bismuth nanoparticles

In a typical synthesis process 6.66mmol $Bi(Cl)_3$,10mmol of Sodium Selenite (Na_2SeO_3), and 0.666g EDTA ethylene diamine tetra acetic disodium salt were mixed with 135 mL distilled water in a 250mL R.B flask. After thorough mixing 1.166g of KOH or NaOH or NH_3, 1.166g ascorbic acid were added to the contents of R.B flask. Contents of the flask were heated in an oil bath at temperature of 150 ^{o}C with constant stirring with a speed of 100 rpm for 24 hrs. The precipitated dark grey powder was filtered, washed with distilled water and ethanol for several times. Then as-obtained air dried sample was calcinated for about 6hrs at 100^{o}C.

Afterwards the sample was characterized by X-ray powder diffraction (XRD), UV-DRS, scanning electron microscopy (SEM), transmittance electron microscopy (TEM).

2.2Characterization techniques

The phase and purity of Bismuth selenide nanostrcutures were determined by X-ray powder diffraction (XRD) using a Rikagu diffractometer (Tokyo, Japan, Cu Kα radiation, λ= 0.1546 nm) radiation in a 2θ range of 10-70º at room temperature running at 40 kV and 40mA. XRD peaks were indexed with the powder X software and the material is confirmed by comparing the XRD results with the standard JCPDS card number. The morphology of the products was examined by transmission electron microscopy (FEI-Model Tecnai G2S Twin - 200 kV)and selected area electron diffraction (SAED) the samples were dispersed in ethanol by ultrasonic treatment and dropped on formvar coated-copper grids. All UV-Vis DRS characterization were recorded under ambient conditions using a Shimadzu 2100 UV-Vis spectrophotometer in the range of 200-800 nm with a scan rate of 60 nm/min (Braeside, Australia with quartz cuvette cells with a 1-cm path length. $BaSO_4$ was used as the reference. The morphology of the products was examined by scanning electron microscopy (SEM, Quanta 200), Elemental analysis was performed by using an EDAX Bruker Nano GmbH, X Flash Detector (Model5010).

2.3PhotodegradationStudy:

The photocatalytic activity was estimated by measuring the percentage decomposition of the dye in an aqueous solution. A known concentration of dye solution was prepared by dissolving (10 mg of dye in one liter of carbonate free double distilled water ((10 mg/L). For a 250 mL of the prepared dye solution, 0.20 g of catalyst was added. The suspension was stirred in the dark for about 1hr to ensure adsorption- desorption equilibrium between the dye and catalyst, prior to UV irradiation. Then the suspension was irradiated with a UV light from a 400-W high-pressure Hg lamp in a UV chamber at 25 $_oC$. This lamp emits an ultra violet radiation of 254 nm. Absorbance (A) of the sample was recorded as a function of time after due centrifugation and filtration through a 0.2- μm pore filter to remove the catalyst particles. The decolorization of the dye was calculated by formula:

$$\text{Degradation efficiency (Decolorization)} = \frac{(C_0 - C)}{C_0}$$

The initial concentration (C_o) and the concentration at a given time (C) are computed from the initial absorbance (A_o) and absorbance at a given time (A) respectively.

The photocatalytic degradation efficiency of the dye solution was calculated with the following formula:

$$\eta = \frac{(A_0 - A)}{A_0}$$

III. Results&Discussions

3.1 XRD Studies :

Figure 1 shows the XRD patterns of the Bi_2Se_3 nanostructure preparedin three different bases (namely KOH, NaOH and NH_4OH) at 150 °C for 48 h. In this pattern, all of the diffraction peaks can be steadily indexed to a rhombohedral geometry phase of Bi_2Se_3 (JCPDS: 33-0214)preferential growth orientation along (015) direction. XRD results reveal that the bismuth selenide nanostructures prepared with KOH exhibit high tendency of acquiring crystalline nature. No peaks forBi_2O_3 or bismuth selenium oxide (Bi_2O_5Se) that could possibly form during the synthesis process, indicating the high purityof the Bi_2Se_3 samples. This procedure enables us to synthesize Bi_2Se_3 nanostructure successfully in thermal method. The crystallite size was determined from the (015) peak using the scherrer's formula and these values presented in the Table 1.

$D=0.94\lambda/ \beta Cos\ \theta$

Table 1: Crystallite size of Bismuth Selenide powder prepared by using various bases.

Material	FWHM (015) peak	Crystallite size(nm)
BSK (KOH)	0.2755	29.53
BSN (NaOH)	0.3542	27.57
BSA (NH3)	0.2362	36.19

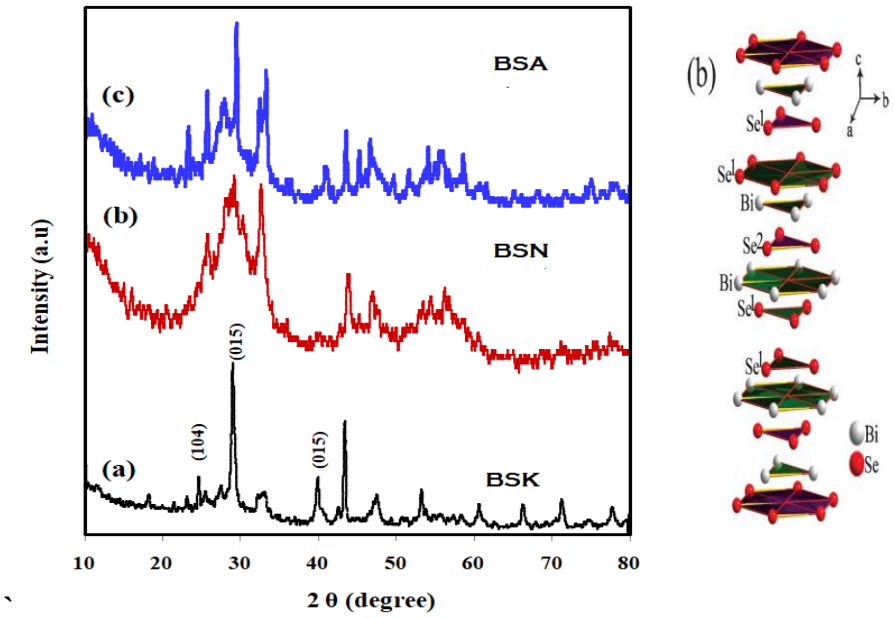

Figure1: *XRD Spectrum*

3.2 UV-DRS :

Figure 2 shows the UV-DRS of Bi_2Se_3 nanostructures synthesized with base KOH ,NH3 and NaOH. UV-Vis spectrum of the prepared compounds were recorded in the range of 250-750 nm. No characteristic absorption peak is observed in UV-Visible range due to the extremely narrow band gap and in the case of BSK nano compound it shows relatively high transmittance than the other two compounds in the graph . The theoretical band gap energy for bulk Bi_2Se_3 is f 0.35 eV [optical] hence the absorption band does not fall in the range of 250-750 nm.

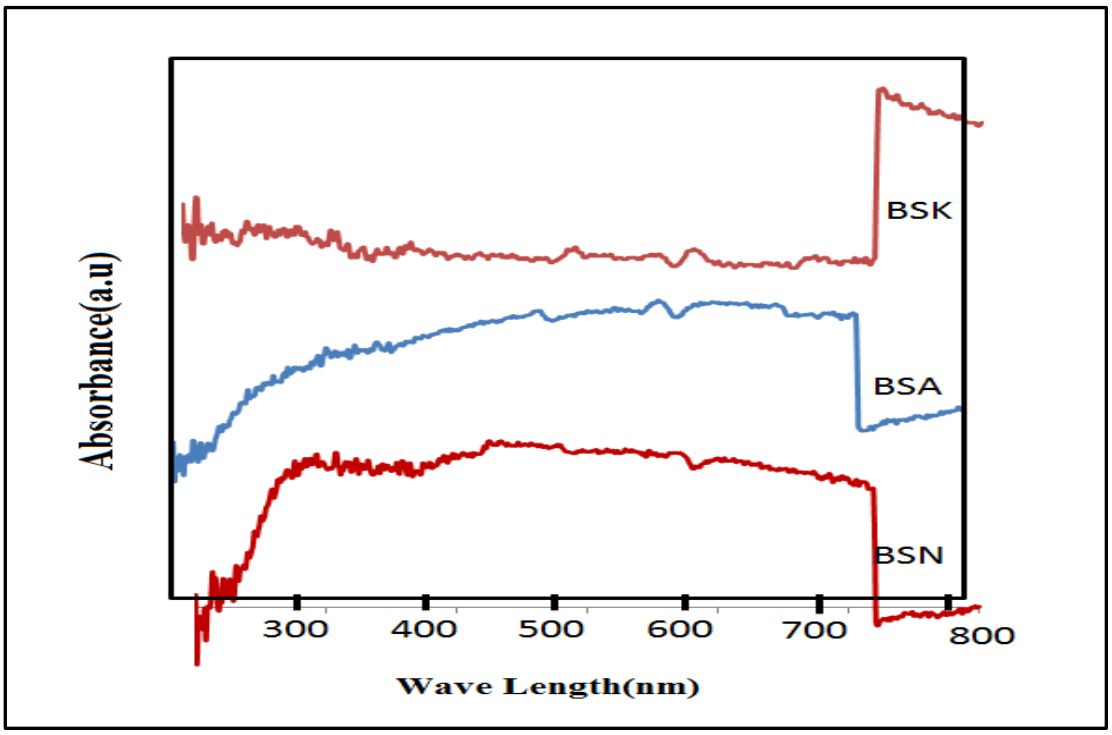

Figure 2: *U.V DRS Spectrum*

3.3 SEM Analysis:

Surface property of the prepared bismuth selenide powder was studied by recording SEM micrographs(Fig.no 3) .Morphology of SEM reveals the form of Bi nanoparticles to nanorods obtained in the range of 10-200nm. With the introduction of different bases the compound resulted in the formation of Bi2Se3 material at nanoscale with different kinds of morphologies. Thus the surface nature of material is influenced by the base employed during the reaction process.

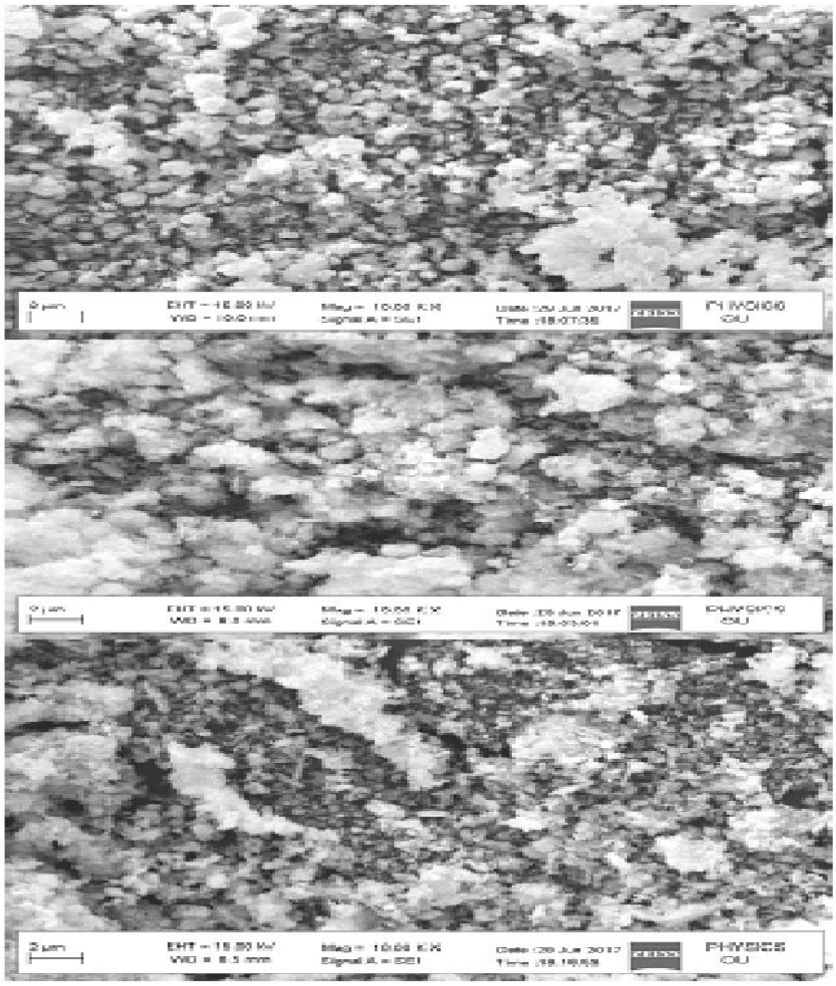

Figure 3*: SEM images of Bi2Se3 nanoflowers to nanopowders*

3.4 Elemental analysis by EDAX :

The quantitative elemental analysis of Bi2Se3 was carried out at room temperature of the composition of Bi_2Se_3 from EDAX. Table No. Presents the elemental theoretically expected stoichiometric composition of Bi_2Se_3 (in terms of atomic %) is Bi= 65, Se= 26. The compound is nonstiochiometric in nature.

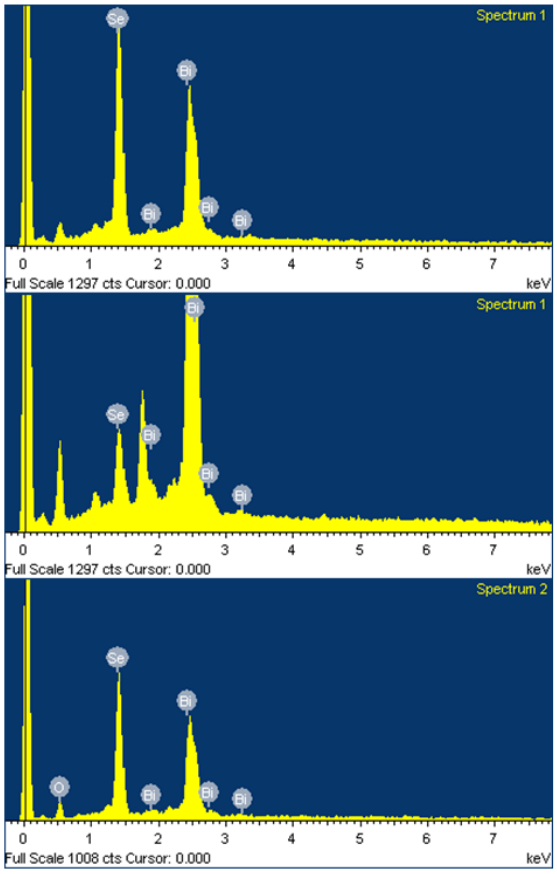

Element	Weight%	Atomic%
Se L	38.22	62.08
Bi M	61.78	37.92
Totals	100.00	

Element	Weight%	Atomic%
Se L	7.91	18.51
Bi M	92.09	81.49
Totals	100.00	

Element	Weight%	Atomic%
O K	10.84	49.49
Se L	33.65	31.11
Bi M	55.51	19.40
Totals	100.00	

Figure 4: *EDAX analysis of Bi_2Se_3*

3.5 TEM analysis:

The TEM images showed that the material has different morphologies with variation of base .

BSK (Catalyst-I) BSN(Catalyst-II) BSA(Catalyst-III)

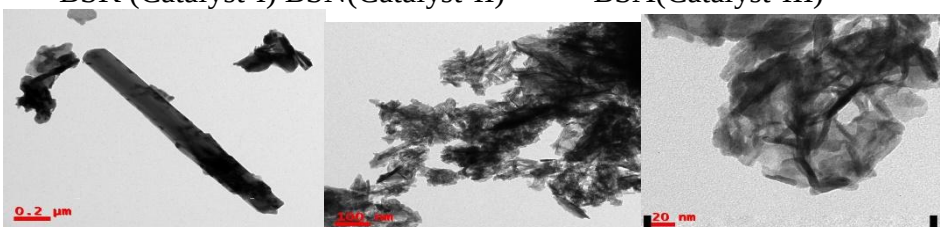

Figure 5:*Tem images of catalyst*

Here in this TEM image showed approximately hexagonal lamellar plates . Based on TEM images it should be pointed out that the morphology of the material is highly influenced by variation of base used during the experiment. During the preparation of the compound by regular laboratory process i.e, solvothermal method we used three different kinds of bases such as KOH, NaOH and NH_3 the images obtained here clearly demonstrates that they have influence on the morphology of the resulting compound.

3.6 Photodegradation of cationic dyes:

Effectofcatalystmorphologyonrateofdyedegradation:

The morphology of catalyst plays an important role in affecting its performance. Inthis present study we have used nanostructured Bi_2Se_3 with three different morphologies forthedegradationofMG.Bi_2Se_3 synthesizedbyusing KOH (catalyst-Ior BSK) ,NaOH (catalyst- IIor BSN) and NH_3(catalyst-IIIor BSA)wereusedforthisstudy.Morphologyof BSK showednanorods with a size in the range of 29nm, while BSN indicated nanotubeswithsize(i.e 27nm) and BSA indicated nanowafers as mentioned in section 3.5

Catalyst - III was found to be more efficient than Catalyst- II and I, for the degradation ofMG. The results clearly indicated that catalytic activity depended on its morphology. Thismight be attributed to an increased surface area from Catalyst-III to Catalyst-II than I, furnishing morespace for adsorptionofthedye.

Table 2: Cationic Dye degradation using Bismuth selenide catalysts

Dye	BSN		BSK		BSA	
	R.T (hrs)	Degradation (%)	R.T (hrs)	Degradation (%)	R.T (hrs)	Degradation (%)
M.G	5.0	40	5.0	61	5.0	83
M.B	5.0	21	5.0	36.4	5.0	28.8
C.V	5.0	83.3	5.0	65	5.0	85
M.V	5.0	75	5.0	52	5.0	70

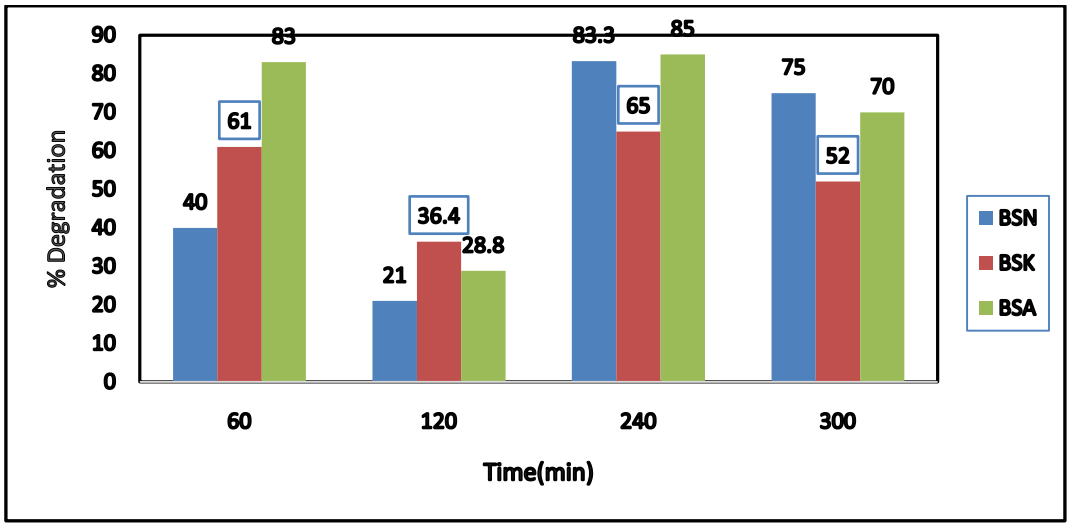

Figure 6: A comparative study of dye degradation using Bi_2Se_3catalysts

Proposed mechanism of dye degradation using Bi_2Se_3

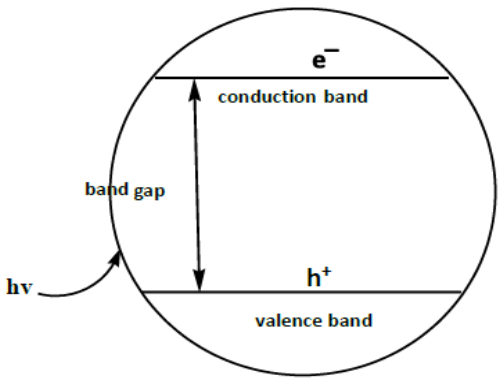

$Bi_2Se_3 \rightarrow (h^+_{VB} + e^-_{CB})\ Bi_2Se_3$ (1)

$H_2O + h^+ \rightarrow H^+ + OH^-$ (2)

$h^+ + OH^- \rightarrow OH^\cdot$ (3)

$OH^\cdot$ + Organic species $\rightarrow$ Products (4)

$e^- + O_2 \rightarrow O^{-}_2$ (5)

O^{-}_2 + Organic species $\rightarrow$ Products (6)

IV. Conclusion

Bi_2Se_3 nanoparticles were synthesized by solvothermal process by variation of base to form BSN, BSK and BSA respectively . The as synthesized Bi_2Se_3nanoparticles were characterized by XRD, SEM, TEM, EDX and UV–Vis spectra. Role of Bi_2Se_3 light enabled photocatalysts were studied through the measurement of degradation efficiencies of cationic dyes such as MG, M.V,C.V and M.B.

References

[1]. S. Garfield, Mauve: How One Man Invented a Color That Changed The World, W. W. Norton & Company, 2002.
[2]. P.F. Gordon, P. Gregory, Organic chemistry in colour, Springer, 1987.
[3]. N.P. Raval, P.U. Shah, N.K. Shah, Malachite Green ''a cationic dye'' and its removal from aqueous solution by adsorption, Appl. Water Sci. 7 (2017) 3407–3445.
[4]. T. Robinson, G. McMullan, R. Marchant, P. Nigam, Remediation of dyes in textile effluent: a critical review on current treatment technologies with a proposed alternative, Bioresour. Technol. 77 (2001) 247–255.
[5]. A. Rogers, Chemistry and the leather industry, J. Chem. Educ. 2 (5) (1925) 363–369.
[6]. S. Ramalingam, R.R. Jonnalagadda, Tailoring nanostructured dyes for auxiliary free sustainable leather dyeing application, ACS Sustain. Chem. Eng. 5 (2017) 5537–5549.
[7]. P. Milvy, K. Kay, Mutagenicity of 19 major graphic arts and printing dyes, J. Toxicol. Environ. Health 4 (1978) 31–36.
[8]. R. Schiek, Paints and pigments, J. Chem. Educ. 57 (4) (1980) 270–271.
[9]. W.C. Holmes, Application of the direct dyes in coloring paper, The, J. Ind. Eng. Chem. 14 (10) (1922) 958–960.
[10]. N. Christensen, Developments in colorants for plastics, Rapra, Rev. Rep. (2000).
[11]. W.F. Bergfeld, D.V. Belsito, J.G. Marks, F.A. Andersen, Safety of ingredients used in cosmetics, J. Am. Acad. Dermatol. (2005) 125–132.
[12]. M. uleková, M. Smrová, A. Hudák, M. He elová, M. Fedorová, Organic colouring agents in the pharmaceutical industry, Folia Veterinaria 61 (3) (2017) 32–46.
[13]. K. Yamjala, M.S. Nainar, N.R. Ramisetti, Methods for the analysis of azo dyes em- ployed in food industry – a review, Food Chem. 192 (2016) 813–8.
[14]. B.K. Mandal, S. Mathiyalagan, R. Dalavai, Y.-C. Ling, Simultaneous identification of synthetic and natural dyes in different food by UPLC-MS, IOP Conf. Series, Mater. Sci. Eng. 263 (2017) 022011 (1–8).
[15]. S. Chowdhury, P. Saha, Adsorption kinetic modeling of safranin onto rice husk biomatrix using pseudo-first and pseudo-second-order kinetic models: comparison of linear and non-linear methods, Clean - Soil, Air, Water 39 (2011) 274–282.
[16]. K.A. Adegoke, O.S. Bello, Dye sequestration using agricultural wastes as adsorbents, Water Resour. Ind. 12 (2015) 8–24.
[17]. X.-F. Lu, H.-R. Ma, Q. Zhang, K. Du, Degradation of methyl orange by UV, O3 and UV/O3systems: analysis of the degradation effects and mineralization mechanism, Res. Chem. Intermed. 39 (2013) 4189–4203.
[18]. Y. Yao, B. He, F. Xu, X. Chen, Equilibrium and kinetic studies of methyl orange adsorption on multiwalled carbon nanotubes, Chem. Eng. J. 170 (2011) 82–89.
[19]. S.P. Raghuvanshi, R. Singh, C.P. Kaushik, Kinetics study of methylene blue dye bioadsorption on baggase, Appl. Ecol. Environ. Res. 2 (2) (2004) 35–43.
[20]. G. Sharma, V.K. Gupta, S. Agarwal, A. Kumar, S. Thakur, D. Pathania, Fabrication and characterization of Fe@MoPO nanoparticles: Ion exchange behavior and photocatalytic activity against malachite green, Journal of Molecular Liquids, 219 (2016) 1137-1143.
[21]. G. Ghosh and B. P. Varma, Thin Solid Films, 1979, 60, 61;M. E. Rincon and P. K. Nair, J. Phys. Chem. Solids, 1996, 57,9137; L. Huang, P. K. Nair and M. T. S. Nair, Thin Solid Films,1995, 268, 49; M. E. Rincon, R. Suarez and P. K. Nair, J. Phys. Chem. Solids, 1996, 57, 9147.
[22]. P. Boudjouk, M. P. Remington, Jr and D. G. Grier, Inorg. Chem.,1998, 37, 3538.
[23]. (a) H. J. Goldsmid, J. Appl. Phys., 1961, 32, 2198; (b) X. B. Zhao,X. H. Ji, Y. H. Zhang, T. J. Zhu, J. P. Tu and X. B. Zhang, Appl.Phys. Lett., 2005, 86, 06211; (c) B. Poudel, Q. Hao, Y. Ma,Y. C. Lan, A. Minnich, X. B.YuYan, D. Z. Wang, A. Muto,F. Vashaee, X. Y. Chen, J. M. Liu, M. S. Dresselhaus, G. Chen and Z. F. Ren, Science, 2008, 320, 63.
[24]. Sun, Y. F.; Cheng, H.; Gao, S.; Liu, Q. H.; Sun, Z. H.; Xiao,C.; Wu, C. Z.; Wei, S. Q.; Xie, Y. Atomically thick bismuthselenide freestanding single layers achieving enhanced thermoelectric energy harvesting. J. Am. Chem. Soc. 2012, 134, 20294−20297.
[25]. Soni, A.; Zhao, Y. Y.; Yu, L. G.; Aik, M. K. K.; Dresselhaus,M. S.; Xiong, Q. H. Enhanced thermoelectric properties of solution grown Bi2Te3–xSex nanoplatelet composites. NanoLett. 2012, 12, 1203−1209. 6. Min, Y.; Roh, J. W.; Yang, H.; Park, M.; Kim, S. I.; Hwang,S.; Lee, S. M.; Lee, K. H.; Jeong, U. Surfactantfree scalable synthesis of Bi2Te3 and Bi2Se3 nanoflakes and enhanced thermoelectric properties of their nanocomposites. Adv.Mater. 2013, 25, 1425−1429.
[26]. Yu, J. K.; Mitrovic, S.; Than, D.; Varghese, J.; Heath, J. R.Reduction of thermal conductivity in phononicnanomeshstructures. Nat. Nanotechnol. 2010, 5, 718−721
[27]. Linder, J.; Yokoyama, T.; Sudbø, A. Anomalous finite size effects on surface states in the topological insulator Bi2Se3.Phys. Rev. B 2009, 80, 205401.
[28]. Yao, J.; Koski, K. J.; Luo, W. D.; Cha, J. J.; Hu, L. B.; Kong,D. S.; Narasimhan, V. K.; Huo, K. F.; Cui, Y. Optical transmission enhancement through chemically tuned two dimensional bismuth chalcogenide nanoplates. Nat. Commun.2014, 5, 5670.
[29]. Min, Y.; Moon, G. D.; Kim, B. S.; Lim, B.; Kim, J. S.; Kang,C. Y.; Jeong, U. Quick, controlled synthesis of ultrathin Bi2Se3 nanodiscs and nanosheets. J. Am. Chem. Soc. 2012,134, 2872−2875.
[30]. Zhang, J.; Peng, Z. P.; Soni, A.; Zhao, Y. Y.; Xiong, Y.;Peng, B.; Wang, J. B.; Dresselhaus, M. S.; Xiong, Q. H.Raman spectroscopy of few-quintuple layer topologicalinsulator Bi2Se3 nanoplatelets. Nano Lett. 2011, 11, 2407−2414

M.Shanti. "Synthesis of Bismuth Selenide nanoparticles and its Photocatalytic activity for the degradation of some textile dyes." *IOSR Journal of Applied Chemistry (IOSR-JAC)*, 16(3), (2023): pp 33-39.